CAV2021
11th International Symposium on Cavitation
May 10-13, 2021, Daejon, Korea

Investigation of the Bubble Collapse Temperature Using a Diffuse Interface Method

Saeed Bidi [1,2]*, Andreas Papoutsakis [1], Phoevos Koukouvinis [1], Manolis Gavaises [1]

[1] School of Mathematics, Computer Sciences & Engineering, City, University of London, UK
[2] Institut Jean le Rond d'Alembert, Sorbonne Université, France

Abstract: The numerical algorithm of the widely used multiphase disequilibrium Diffuse Interface Methods (DIMs) such as [1]–[3] is strongly affected by the choice of the Equation of State (EoS), especially in the relaxation step. The scope of this study is to develop an algorithm for a DIM [1] entirely independent of the thermodynamic closure, without solver modification, using a general tabulated form instead of parametric EoSs (PEoS). The algorithm facilitates the use of any arbitrary EoS through tabulated data. Nevertheless, since the aim of the current study is only to develop the algorithm, the data for the tabulated EoS (TEoS) are extracted from the applied PEoSs, i.e. stiffened gas for water and ideal gas for air. The comparison of the results for the simulation of the spherical bubble collapse with both the TEoS and PEoS is employed as a measure to assess the TEoS algorithm. The results obtained with both implementations are compared with the Keller-Miksis model. Moreover, the spatio-temporal distribution of the temperature in the bubble interior and the liquid in the vicinity of the bubble is investigated.

Keywords: CFD; Multiphase; Bubble collapse; Thermodynamics; Thermal effects; Tabulated EoS

1. Introduction

Extremely high pressure and temperature of a collapsing bubble are the key features of a violent implosion, where complex phenomena such as sonoluminescence and chemical reactions are observed. A consequence of the very high temperature is the generation of free radicals responsible for radical stress in biological systems during ultrasound treatment [4]. They also play a crucial role in pathogenesis and pathological conditions associated with apoptosis and inflammation [5]. An advanced description of the hydrodynamics and thermodynamics of the bubble is essential to analyse the free radical formation.

Multiphase Computational Fluid Dynamics (CFD) solvers have been widely used to simulate bubble collapse by interface tracking or capturing methods. However, the vast majority of the published literature deals with Stiffened Gas Equation of State (SG EoS) and Ideal Gas Equation of State (IG EoS) [6]–[8]. It is known, however, that the IG EoS overestimates the temperatures during bubble collapse [9]. Only a handful of works discuss non-ideal effects in bubble collapse e.g. [10] which are often constrained to 1-D bubble dynamic models such as Rayleigh-Plesset and Keller-Miksis models. In this regard, a realistic gas EoS includes complex phenomena such as ionization and dissociation that increase the specific heat of the gas resulting in lower temperatures during the adiabatic compression.

Most studies with the DIMs have been limited to the IG EoS and SG EoS to avoid the complexities posed by more advanced EoS. In this work, an EoS-independent formulation is proposed with which any arbitrary EoS can be used through tabulated data.

2. Materials and Methods

In the present study, the relaxation multiphase DIM [1] is adopted as follows:

$$\frac{\partial \boldsymbol{U}}{\partial t} + \frac{\partial \boldsymbol{F}}{\partial x} + \boldsymbol{H}\frac{\partial u}{\partial x} = \boldsymbol{R}, \tag{1}$$

* Corresponding Author: S. Bidi, saeed.bidi@city.ac.uk

in which:

$$\boldsymbol{U} = ((\alpha\rho)_1, (\alpha\rho)_2, \rho u, \rho E, \alpha_1, \alpha_1\rho_1 e_1, \alpha_2\rho_2 e_2)^T,$$
$$\boldsymbol{F} = \big((\alpha\rho)_1 u, (\alpha\rho)_2 u, \rho u^2 + (\alpha_1 p_1 + \alpha_2 p_2), \big(\rho E + (\alpha_1 p_1 + \alpha_2 p_2)\big)u, \alpha_1 u, \alpha_1\rho_1 e_1 u, \alpha_2\rho_2 e_2 u\big)^T,$$
$$\boldsymbol{H} = (0,0,0,0, -\alpha_1, \alpha_1 p_1, \alpha_2 p_2)^T,$$
$$\boldsymbol{R} = (0,0,0,0, \mu(p_1 - p_2), -p_I\mu(p_1 - p_2), p_I\mu(p_1 - p_2))^T,$$

where the following notation is used: x (coordinate), t (time), ρ (density), p (pressure), α (volume fraction), u (velocity), e (specific internal energy), p_I (interfacial pressure), and μ (relaxation coefficient).

The SG EoS and IG EoS are considered for the liquid and gas, respectively, as described in [1]. Although the final aim of implementation of the EoS-independent formulation is to use more advanced EoS, the tables in this study are generated using the SG EoS and IG EoS. In this way, similar results will demonstrate the successful tabulated approach. The table consists of pressure and temperature as the inputs and the desired variables are computed with bilinear interpolation at each stage.

2.1. Hyperbolic step

In this step, Eq. (1) is solved in the absence of the relaxation terms within the Finite Volume framework [11] for adaptive hybrid unstructured grids [12]. The Godunov method is used with the MUSCL scheme for the face reconstruction and the HLLC as the approximate Riemann solver.

2.2. Relaxation step

The phasic volume fraction and density are adapted in the relaxation step to ensure the mechanical equilibrium by solving Eq. (1) without the convection terms which after some manipulations reads:

$$e_k^{(2)} - e_k^{(1)} - p^{(2)}\left(\frac{1}{\rho_k^{(2)}} - \frac{1}{\rho_k^{(1)}}\right) = 0,$$
$$\frac{(\alpha_1\rho_1)^{(1)}}{\rho_1^{(2)}} + \frac{(\alpha_2\rho_2)^{(1)}}{\rho_2^{(2)}} - 1 = 0, \qquad (2)$$

where the superscripts (1) and (2) show the values from the previous hyperbolic step and after the relaxation step, respectively, for component k. If the PEoSs are used, the internal energy can be expressed by the pressure and density of the components. In the case of the TEoSs, there is no mathematical expression to relate the internal energies to pressure and densities. Therefore, the left-hand side of the system of Eq. (2) is considered as the error function for an iterative solution. Providing an initial guess for the temperatures and pressure of the system, it is solved iteratively through the multi-variable Newton method for pressure and temperatures. The values of the density and internal energy are interpolated through the tabulated data.

2.3. Re-initialization step

There is no guarantee, however, that the calculated pressure in the relaxation step is corresponding to the mixture EoS. Therefore, re-initialization is performed as the third step in which the pressure is calculated using the mixture internal energy $\rho e = \alpha_1\rho_1 e_1 + \alpha_2\rho_2 e_2$ where the left-hand side is computed from the total energy equation $\rho e = \rho E - \frac{1}{2}\rho u^2$. In this way, the new pressure respects the total energy conservation. In the case of using the SG EoS and IG EoS, it reads:

* Corresponding Author: S. Bidi, saeed.bidi@city.ac.uk

$$p(\rho, e, \alpha_1, \alpha_2) = \frac{\rho e - \left(\frac{\alpha_1 \gamma_1 p_{\infty,1}}{\gamma_1 - 1} + \frac{\alpha_2 \gamma_2 p_{\infty,2}}{\gamma_2 - 1}\right)}{\frac{\alpha_1}{\gamma_1 - 1} + \frac{\alpha_2}{\gamma_2 - 1}}. \quad (3)$$

If the TEoS is considered, however, deriving a similar equation to Eq. (3) is not possible. Therefore, the mixture internal energy equation is solved iteratively for the pressure and internal energies.

3. Results

The symmetric collapse of an air bubble surrounded by high pressure water is considered to assess the performance of the numerical method. Each phase contains a very small value of the opposite phase volume fraction $\varepsilon = 10^{-6}$ to keep the system hyperbolic [1]. The simulation is done in 1D spherical coordinate with the total 250 elements, $3N_{R0} = 150$ of which are uniformly placed in $[0,3R_0]$ where N_{R0} denotes the number of cells per initial radius R_0. The rest of elements are uniformly distributed in $(3R_0, 20R_0]$. The monotonized central slop limiter is used for the MUSCL reconstruction scheme. Reflective and transmissive boundary conditions are used for the left ($r = 0\ mm$) and right ($r = 20R_0$) boundaries, respectively. Also, a two-step time integration method [6] has been used with a varying time step based on the CFL number set to 0.1. Initially, the bubble has a uniform pressure p_a while the surrounding pressure increases gradually towards the far-field p_f:

$$p_w(r) = p_f + \frac{R_0}{r}(p_a - p_f). \quad (4)$$

The initial condition for the bubble collapse is provided in Table 1. The temperature is initially equal in both phases.

Table 1. Initial conditions for the bubble collapse

p_a (Pa)	p_f (Pa)	$\rho_a \left(\frac{kg}{m^3}\right)$	$\rho_w \left(\frac{kg}{m^3}\right)$
1.01325×10^5	3.57589×10^7	1.225	1.0114×10^3

A comparison between the results and the Keller-Miksis model is shown in Figure 1 (a). It is observed that the present method captures the compression and expansion rate with high accuracy. Similar results with the TEoSs and PEoSs indicate that the TEoS implementation has been successful. The temperature distribution in $r = [0, R_0]$ is also depicted in Figure 1 (b). As the bubble approaches to collapse, the temperature increases mainly due to the very high compression rate and reaches the maximum value of $\cong$ 10000 K in collapse which is noticeably higher than the value that a real gas EoS such as the Peng-Robinson EoS is expected to predict $\cong$ 6000 K by introducing the real gas effects. Nevertheless, the temperature is quenched rapidly as soon as the hydrodynamic expansion starts.

4. Conclusion

The EoS plays a crucial role in the numerical implementation of the DIM, particularly in the relaxation and re-initialization steps. The tabulated approach described in this study empowers the DIM to benefit from more complex parametric or empirical equations of state with no required modification. Identical results with tabulated and parametric forms of the IG EoS and SG EoS demonstrate the applicability of the algorithm. Advanced real gas EoSs will be implemented in the tabulated form in our further studies to investigate the bubble collapse temperature.

* Corresponding Author: S. Bidi, saeed.bidi@city.ac.uk

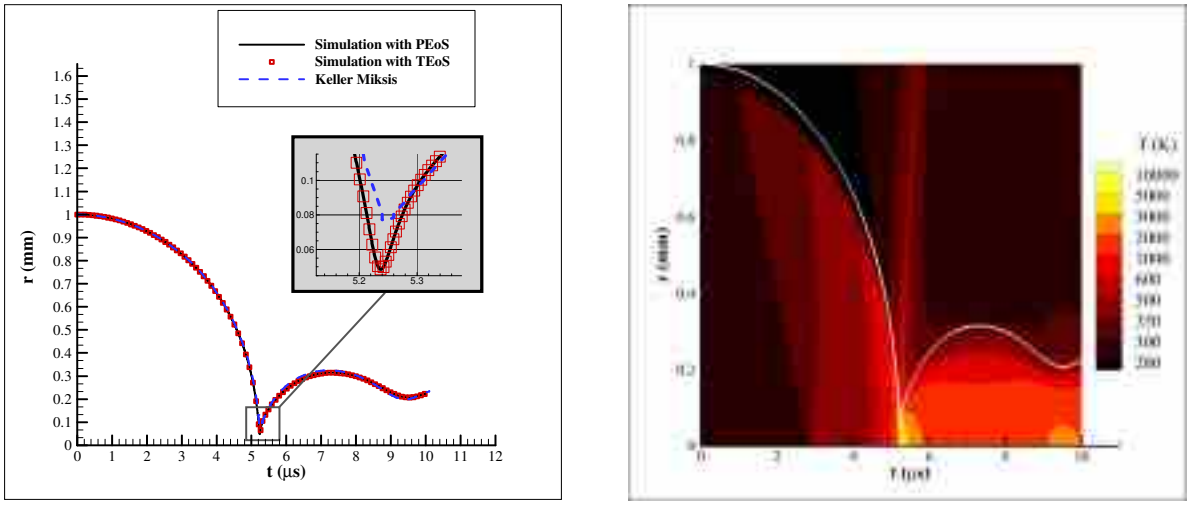

(**a**) (**b**)

Figure 1. Comparison of the numerical results with the Keller-Miksis model (a) high; (b) spatio-temporal evolution of bubble temperature with radius change in time (white line).

Acknowledgments: This project has received funding from the European Union Horizon-2020 Research and Innovation Programme, Grant Agreement No. 813766.

References

[1] Richard Saurel, F. Petitpas, and R. A. Berry, "Simple and efficient relaxation methods for interfaces separating compressible fluids, cavitating flows and shocks in multiphase mixtures," *J. Comput. Phys.*, vol. 228, no. 5, pp. 1678–1712, 2009.

[2] M. Pelanti and K. M. Shyue, "A mixture-energy-consistent six-equation two-phase numerical model for fluids with interfaces, cavitation and evaporation waves," *J. Comput. Phys.*, vol. 259, pp. 331–357, 2014.

[3] A. Zein, M. Hantke, and G. Warnecke, "Modeling phase transition for compressible two-phase flows applied to metastable liquids," *J. Comput. Phys.*, vol. 229, no. 8, pp. 2964–2998, 2010.

[4] Y. Kung *et al.*, "A Single High-Intensity Shock Wave Pulse With Microbubbles Opens the Blood-Brain Barrier in Rats," *Front. Bioeng. Biotechnol.*, vol. 8, no. May, 2020.

[5] B. Fubini and A. Hubbard, "Reactive oxygen species (ROS) and reactive nitrogen species (RNS) generation by silica in inflammation and fibrosis," *Free Radic. Biol. Med.*, vol. 34, no. 12, pp. 1507–1516, 2003.

[6] K. Schmidmayer, S. H. Bryngelson, and T. Colonius, "An assessment of multicomponent flow models and interface capturing schemes for spherical bubble dynamics," *J. Comput. Phys.*, vol. 402, 2020.

[7] N. Bempedelis and Y. Ventikos, "A simplified approach for simulations of multidimensional compressible multicomponent flows: The grid-aligned ghost fluid method," *J. Comput. Phys.*, vol. 405, pp. 1–32, 2020.

[8] A. Zein, M. Hantke, and G. Warnecke, "On the modeling and simulation of a laser-induced cavitation bubble," *Int. J. Numer. Methods Fluids*, vol. 73, no. 2, pp. 172–203, 2013.

[9] K. Kerboua and O. Hamdaoui, "Influence of reactions heats on variation of radius, temperature, pressure and chemical species amounts within a single acoustic cavitation bubble," *Ultrason. Sonochem.*, vol. 41, pp. 449–457, 2018.

[10] D. Schanz, B. Metten, T. Kurz, and W. Lauterborn, "Molecular dynamics simulations of cavitation bubble collapse and sonoluminescence," *New J. Phys.*, vol. 14, 2012.

[11] A. Papoutsakis and M. Gavaises, "Numerical investigation of Fluid Structure Interaction in elastic soft matter using a diffused interface approach," *3rd Int. Conf. INTERFACIAL Phenom. Heat-mass-trans.*, 2020.

[12] A. Papoutsakis, P. Koukouvinis, and M. Gavaises, "Solution of cavitating compressible flows using Discontinuous Galerkin discretisation," *J. Comput. Phys.*, vol. 410, p. 109377, 2020.

* Corresponding Author: S. Bidi, saeed.bidi@city.ac.uk